Learning Identification Control for Model-Based Optoelectronic Packaging

Shubham K. Bhat, Timothy P. Kurzweg, *Member, IEEE*, and Allon Guez

***Abstract*—In this paper, we present a learning control algorithm for the packaging automation of optoelectronic systems. This automation provides high performance, low-cost alignment and packaging through the use of a model-based control theory and system-level modeling. The approach is to build an *a priori* model, specific to the assembled package's optical power propagation characteristics. From this model, an inverse model is created and used in the "feedforward" loop. In addition to this feedforward model, the controller is designed with feedback components, along with the inclusion of a built-in optical power sensor. We introduce a learning technique, which is activated at a lower sampling frequency for specific and appropriate tasks, to improve the model used in the model-based control. Initial results are presented from an experimental test bed that is used to verify the control and learning algorithms.**

***Index Terms*—Alignment, learning model identification, optical automation, optical microsystems, packaging.**

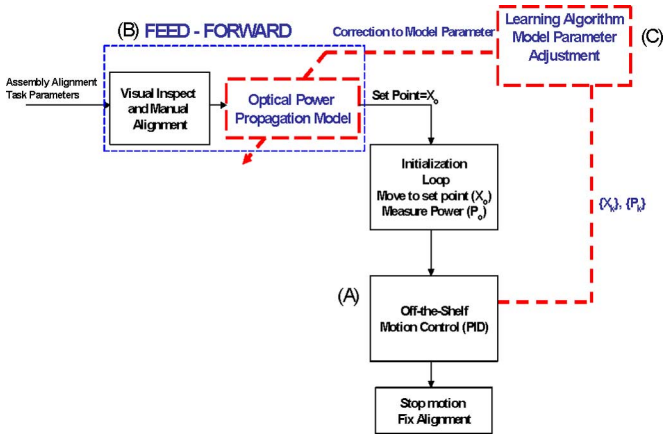

Fig. 1. Model-based control algorithm for automation of photonic systems.

I. Introduction

THERE is a growing interest in the development of automation techniques for photonic alignment and packaging, as the optical microsystem industry desires the benefits of automation experienced by the semiconductor industry. However, the inherent challenges of optoelectronic systems make high-performance automation difficult. In earlier research, an automation process was introduced for the assembly, manufacturing, and packaging of optical microsystems using advanced device-specific optical power models as well as intelligent control theory to yield high performance, low-cost packaging [13]. The *a priori* device knowledge is exploited in online control loops to align optical components in a near optimal configuration to maximize power transmission. The present paper uses a technique that incorporates the materials and mechanics in order to position the components and devices, exerting forces on the various degrees of freedom before, during, and after alignment so that the optical signal is positioned for maximum transmission in a robust manner. This technique provides better performance than the current state of the art, as the alignment is achieved for the global maximum of the system, instead of a local maximum.

For the automation to obtain high performance, the model must be accurate. However, this is not always the case as there could be possible errors in modeling or all of the system parameters might not be known. Even after the packaging is completed, there still remain the issues of postalignment robustness. For example, attaching fibers to a chip requires it to withstand high temperatures and vibrations. The bond needs to remain stable (no temporal changes and no short-term aging) even when high laser power is launched in the fibers [4], [9], [10]. To solve all the above complex, nonlinear problems characterized by a high level of uncertainty, an online learning automaton system is required. This system should provide a capability to adjust the knowledge-based model online, on the basis of the environment response.

The present paper focuses on a learning identification technique in which the system can "learn" and increase the accuracy of the model-based control. This technique provides opportunities for the system to improve upon its power model and adjust its accuracy on the basis of "experienced evidence" or a mismatch between expected power and measured power at a specific axes configuration. This learning technique will decrease the packaging time and hence increase the yield. As device and system designs become more complex, the advantages of this technique will be magnified.

In this paper, brief details of the model-based control technique are provided along with a hardware implementation. The theory behind the most recent research is presented. The paper focuses on the details of the learning model identification scheme, as well as demonstrates the advantages of this technique over the conventional state-of-the-art gradient ascent technique. The paper concludes with future research directions.

II. Automation Control Loops

The control loops used to implement the model-based control algorithm for the automation of photonic devices are presented in Fig. 1. The inner loop, denoted (A) in the figure, is an off-the-shelf servo feedback loop, typically a proportional–integral–differential (PID) controller. The servo loop is initialized with a

Manuscript received September 6, 2005.

The authors are with the Department of Electrical and Computer Engineering, Drexel University, Philadelphia, PA 19104-2816 USA (e-mail: skb25@drexel.edu; kurzweg@ece.drexel.edu; guezal@drexel.edu).

Digital Object Identifier 10.1109/JSTQE.2006.881875

"smart" set point to track x_o, determined from the "feedforward" loop, which is denoted as loop (B) in Fig. 1.

The combination of these two loops defines model-based control, which is the essence of our research design [13]. The feedforward element is typically based upon *a priori* knowledge regarding the process to be controlled [1], [7], [8]. In the present case, this feedforward loop models the optical system alignment and predicts the best point of attachment.

To effectively use the model-based control, models of the control plant $\hat{P}$ and its inverse $\hat{P}^{-1}$ must be determined for the feedforward loop. If done accurately, the feedforward control loop can position the mechanics in the vicinity of the globally optimal configuration. If $\hat{P} = P$, where P is the actual behavior of the plant, perfect tracking can be obtained [13].

To optically model the control plant $\hat{P}$, the angular spectrum technique is used, due to its accuracy and computational efficiency [6], [12]. The angular spectrum technique is an exact solution to the Rayleigh–Sommerfeld formulation, a scalar modeling technique without near- and far-field approximations. The technique is implemented by performing a Fourier transform on the complex optical wavefront transforming from the spatial domain to the frequency domain, multiplying these frequencies by a transfer function describing the propagation medium, and returning to the spatial domain with the use of an inverse Fourier transform. However, there are possible sources of error in this optical modeling technique. The first is the use of a discrete Fourier transform in place of a continuous Fourier expression. Other errors can be found because of aliasing and sampling conditions. Details of these possible errors have been discussed in [11].

In addition to these modeling errors, all of the system parameter information is often not available. In such a case, a system model must be approximately determined from experimental measurements of available inputs and outputs. However, when the structure of the system is known, but certain parameter values are unknown, the system-modeling problem is reduced to the problem of solving, or identifying the unknown parameters [2]. Most current identification techniques consist of reducing the problem to an online parameter identification, which is the focus of this paper.

Loops A and B have been introduced earlier, as in [13]. In this paper, the focus will be on the third and the final loop of this system. This loop is called the "learning loop" and is denoted (C) in Fig. 1. This loop will be discussed in detail in this paper.

III. Learning Model Identification Theory

The existing identification techniques can be classified in several ways. Any identification technique, which uses the input–output signals, available during normal system operation, and identifies a model in real time, is called an online scheme [2]. Offline schemes may use normal operating signals that have been collected and recorded for later analysis. That is, the real-time restriction is relaxed. In the other offline techniques, the normal operating signals are not used, but rather, special test inputs are used instead.

The degree of ignorance about the system and measurements on the system may be described in probabilistic terms. Many current identification techniques depend upon the theory of random processes and are classified as stochastic identification techniques. Alternatively, if the measurement errors and the uncertainties are treated as deterministic errors, then the corresponding identification techniques are deterministic.

A system is identified when the error between the real system and the model is reduced to an acceptable level. If the input to the real system is measured and used as an input to a mathematical model, then the difference between the system and the model outputs is the reduced error. The output error can then be used to adjust the model parameters and thus reduce the output error [2]. The general online learning technique is discussed next. The learning model identification gets activated at a lower sampling frequency for specific and appropriate tasks.

The system to be identified is assumed to be described by $\dot{y} = f(y, u, \beta)$, where y is the output, u is the input, $\dot{y}$ is the differential of the output, and β is a vector of all the unknown parameters. A mathematical model with the same form, with estimated parameter values $\hat{\beta}$, is used as a learning model, such that $\dot{\hat{y}} = f(\hat{y}, u, \hat{\beta})$, where $\hat{y}$ is the estimate of the output, and $\hat{\beta}$ is the estimate of the vector of unknown parameters. The output error vector, e, is defined as $e = y - \hat{y}$. The goal of the learning loop is to manipulate $\hat{\beta}$ such that the error is equal to zero. The implicit assumption is that e is determined entirely by $\hat{\beta}$ and is zero when $\hat{\beta} = \beta$. It follows that $e = e(\hat{\beta})$ and $\dot{e} = (\frac{\partial e}{\partial \hat{\beta}})\dot{\hat{\beta}}$.

The Lyapunov function $v(e)$ is used to determine the stability of the system. In this case, $v(e)$ is selected as a positive definite function of e (i.e., if $v(0) = 0$ then $v(e)0 >$ for all $e \neq 0$) and is defined as $v(e) = \frac{1}{2}e^T Qe$, where Q is a symmetric matrix.

Therefore, the derivative of the function is $\dot{\nu}(e) = e^T Q \frac{\partial e}{\partial \hat{\beta}}\dot{\hat{\beta}}$. If $\dot{\nu}(e)$ could be made negative definite (i.e., if $v(0) = 0$ then $v(e) < 0$ for all $e \neq 0$) by properly choosing $\dot{\hat{\beta}}$, then e would approach zero asymptotically. Selecting $\dot{\hat{\beta}} = -\varepsilon(\frac{\partial e}{\partial \hat{\beta}})^T Qe$, with ε as a positive scalar constant, gives a negative semidefinite (i.e., $v(e) \leq 0$ for all $e \neq 0$) expression $\dot{\nu}(e) = -\varepsilon e^T Q(\frac{\partial e}{\partial \hat{\beta}})(\frac{\partial e}{\partial \hat{\beta}})^T Qe$. Even though not negative definite, this learning model technique is capable of providing system identification in many cases [2].

Before this scheme can be implemented, the sensitivity matrix $\frac{\partial e}{\partial \hat{\beta}}$ must be computed. y does not depend on $\hat{\beta}$, therefore, $\frac{\partial e}{\partial \beta} = -\frac{\partial \hat{y}}{\partial \hat{\beta}} \cong S$. Since the initial conditions for the model $\hat{y}(0)$ can be selected independently of $\hat{\beta}(0)$, the initial condition for the sensitivity matrix S is $S(0) = 0$. The learning model adjustment scheme [2] consists of assuming the initial values for $\hat{\beta}(0)$, adjoining the sensitivity equations to the model equations and using $\dot{\hat{\beta}} = -\varepsilon S^T Qe$. The learning model identification technique can be seen as a control diagram in Fig. 2.

As in all gradient adjustment schemes, the parameter ε must be properly selected. If ε is too large, the schemes will diverge, and if ε is too small, then $\hat{\beta}$ will approach β very slowly. The general conditions under which this technique converges

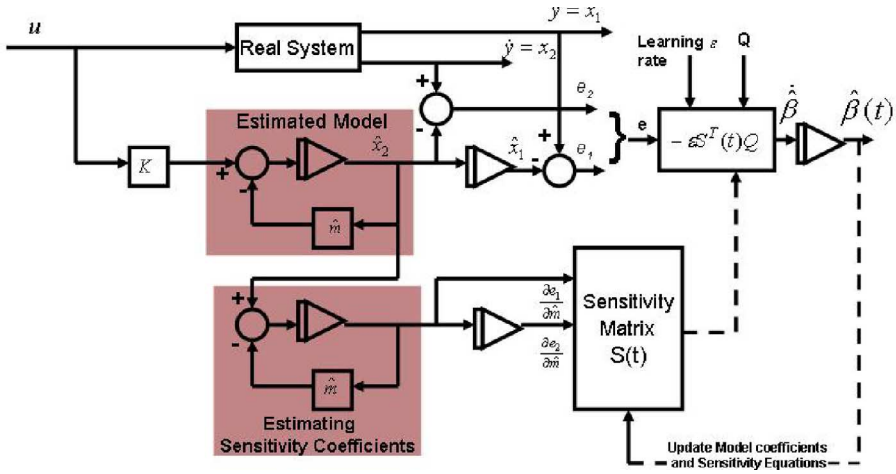

Fig. 2. Simulation of the learning loop technique [2].

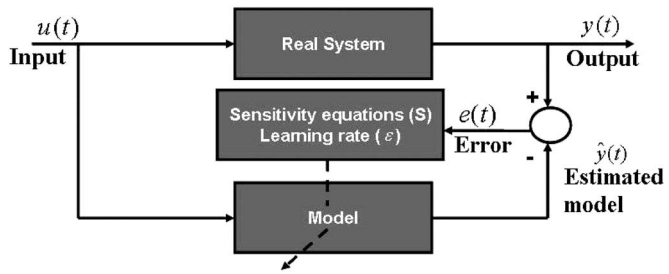

Fig. 3. Learning model identification technique.

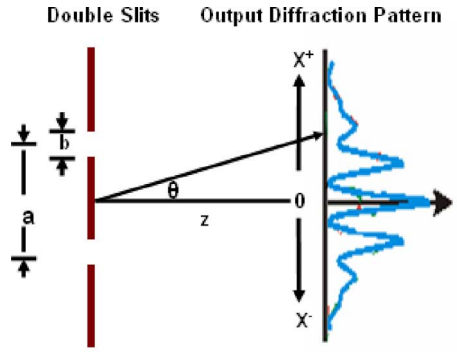

Fig. 4. Double-slit example.

are difficult to determine analytically [3]. The selection of a suitable ε and the weighting matrix Q are determined by a trial-and-error process.

To show an example of this learning identification theory, a one unknown parameter linear system having an input–output differential equation $\ddot{y} + m\dot{y} = Ku$ is presented. In this case, the parameter K is known and the parameter m is unknown (i.e., needs to be learned), and the variables u (input), y (output), and $\dot{y}$ (derivative of the output) can be measured. An estimated model is assumed as $\hat{\ddot{y}} + \hat{m}\hat{\dot{y}} = K\hat{u}$, where "^" represents the estimated parameter. Using the general learning model identification theory (Fig. 3) explained earlier, the equations necessary to implement the learning scheme are the sensitivity coefficients as contained in $S = [\frac{\partial e}{\partial \hat{m}}]$, where $e = [y - \hat{y}]^T$, and $\frac{\partial e}{\partial \hat{m}} = -\frac{\partial \hat{y}}{\partial \hat{m}}$. Next, this learning identification technique is implemented on a specific optoelectronic system example.

IV. Implementation of Learning Identification

In this example, we simulate an optical system comprising an optical fiber coupled to a laser source. The laser source emits a Gaussian beam that passes through two long slits of width b and center-to-center separation a, as seen in Fig. 4. The wavelength of light is given by λ, and $k = \frac{2\pi}{\lambda}$ is the wavenumber associated with the wavelength. The distance of propagation is given by z. In this case, we know the values of b and z to be 18 and 1000 μm, respectively, and we estimate the unknown value of a to be 72 μm.

For the double-slit aperture, the irradiance at any point x in space is given as

$$I(x) = A\,\mathrm{sinc}^2\left(\frac{kb}{2}\sin\left(\tan^{-1}\left(\frac{x}{z}\right)\right)\right) \times \cos^2\left(\frac{ka}{2}\sin\left(\tan^{-1}\left(\frac{x}{z}\right)\right)\right). \quad (1)$$

In order to implement the learning identification technique for identifying the parameter "a," we need to obtain the linear differential form of (1), as seen in Section III ($\ddot{y} + m\dot{y} = Ku$). Hence, we rewrite (1) as

$$I(x) = A_0\,\cos^2\left(\frac{ka}{2}\sin\left(\tan^{-1}\left(\frac{x}{z}\right)\right)\right) \quad (2)$$

where

$$A_0 = A\,\mathrm{sinc}^2\left(\frac{kb}{2}\sin\left(\tan^{-1}\left(\frac{x}{z}\right)\right)\right).$$

Simplifying (2), we obtain

$$I(x) = A_0\cos^2(K_0 a) \quad (3)$$

where

$$K_0 = \frac{k}{2}\sin\left(\tan^{-1}\left(\frac{x}{z}\right)\right).$$

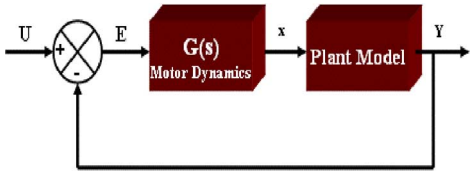

Fig. 5. Control block diagram.

Substituting $K_0 a = \alpha$, and expanding (3) in the neighborhood of a, we get

$$\cos^2(\alpha) = \cos^2(a) - 2\sin(a)\cos(a)(\alpha - a)$$
$$= \cos^2(a)\left\{1 - \frac{\sin(2a)(\alpha - a)}{\cos^2(a)}\right\}. \quad (4)$$

Rewriting $\cos^2(a) = n$; $\sin(2a) = r$, we obtain a linearized equation with α as the argument. Equation (4) becomes

$$\cos^2(\alpha) = n\left\{1 - \frac{r(\alpha - a)}{n}\right\}$$
$$= -r(\alpha) + (n + ra). \quad (5)$$

Substituting (5) in (3), we get

$$I(x) = A_0\cos^2(\alpha) = -A_0 r(\alpha) + A_0(n + ra). \quad (6)$$

This is in the form of a straight line, where the slope is $-A_0 r$ and the intercept is $A_0(n + ra)$. Substituting the initial estimated value of a, and the known values b and z as 72, 18, and 1000 μm, respectively, we obtain

$$I(x) = A_0\cos^2(\alpha) = -1.34\alpha + 27.07. \quad (7)$$

Using (7) in the plant model of the control system, as seen in Fig. 5, we calculate the state-space differential equation for the system. The nonhomogenous state equation is described as

$$G(s) = \frac{X}{U - Y}$$

where $G(s) = \frac{1}{s+1}$ is the motor dynamics, X is the alignment position, and Y is the output light irradiance. Solving the state equation (given earlier), we get $sX + X = U - Y$. Substituting the value of the irradiance from (7) for Y, assuming unity input, and by taking the inverse Laplace transform, we obtain the linear equation

$$\frac{\partial X}{\partial t} = -0.34X + 27.07. \quad (8)$$

Substituting $\dot{y}_1 = X$ and $\ddot{y}_1 = \frac{\partial X}{\partial t}$ and rewriting (8), we get

$$\ddot{y}_1 = -0.34\dot{y}_1 + 27.07. \quad (9)$$

Relating (9) and the general linear differential equation $\ddot{y} + m\dot{y} = Ku$ seen in Section III, we start with the estimated value of the parameter "m" as 0.34, and the known value of the parameter "K" as 27.07.

We now simulate the system, and try to learn "a," which is the center-to-center separation between the slits and has an initial estimate of 72 μm. This initial estimate leads to an initial guess of 0.34 for the parameter "m." The relation between "m" and "a" is given as $m + 1 = -A_o r$, where $r = \sin 2a$ and can be obtained from (4) and (6). By a proper selection of ε, and implementing the learning algorithm, "m" is tracked and shown to converge to its actual value of 1.86, as seen in Fig. 6. The final tracked value of "m" of 1.86 corresponds to a value of 32 μm for "a," the center-to-center separation between the slits. Fig. 7 shows the light intensity profiles formed with the estimated model parameters and the learned parameter values, as obtained by the implementation of the learning identification technique. The waveform marked as "initial guess" represents the estimated plant response obtained using guessed "m" and known "K" values, while the waveform marked as "learned value" represents the actual plant response, which was tracked.

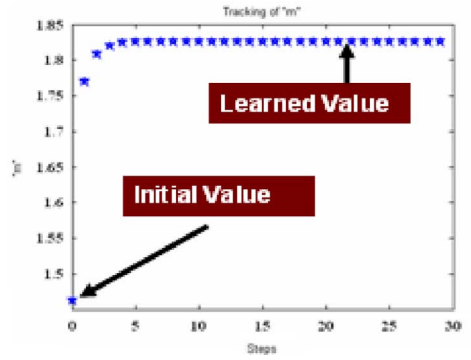

Fig. 6. Learning identification of an unknown variable.

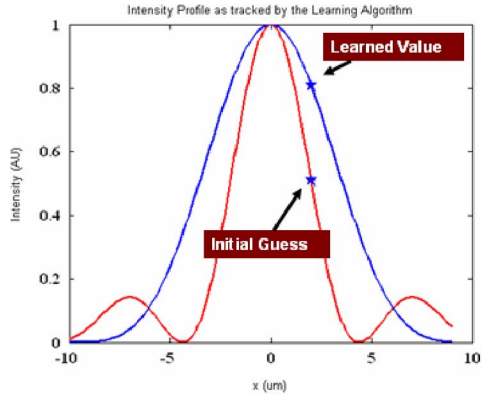

Fig. 7. Learning identification technique.

It may be recalled that the accuracy and convergence of the tracking depend on the parameter ε, and in this case, it was selected as 0.001. In Sections V–VII, the hardware setup and the experimental results are presented.

V. Hardware Setup

To demonstrate the advantages of the automation technique, a test bed has been constructed for the experimental validation of the algorithms. Kulicke and Soffa, Inc., a world leader in automation equipment, has donated an XY table along with the required servomotors, encoders, amplifiers, and a digital-signal-processor (DSP)-based motion controller board from Precision

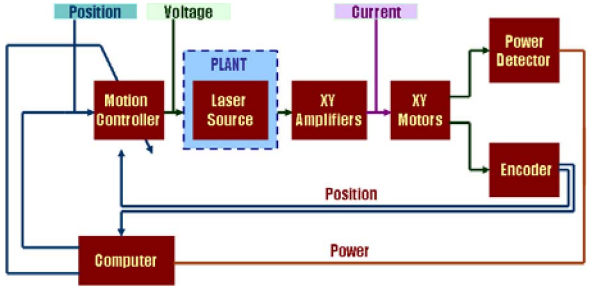

Fig. 8. Hardware setup.

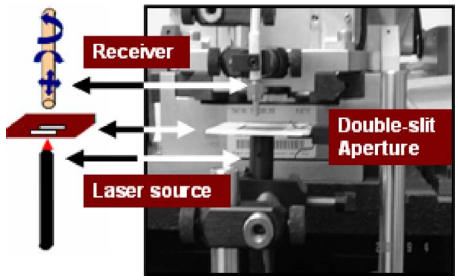

Fig. 9. Laser source being coupled to a fiber through a double slit.

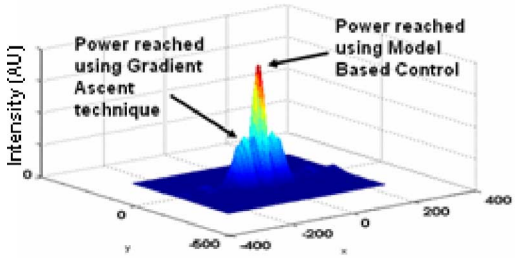

Fig. 10. Diffraction intensity pattern for double slit.

Microdynamics, Inc. for experimental verification of this research. The hardware setup is shown in Fig. 8. The MC8000 motion-control board uses a 32-bit floating-point DSP that performs path planning, feedback regulation, and other real-time computations, freeing the host personal computer (PC) for process application. The card supports data rates with the host PC as high as 7.2 Mb/s.

The motion-control card receives position commands issued by the PC software, from the feedforward control loop. The computer calculates a series of positions for each axis along the desired path at the desired speed set by the feedforward loop. The motion-control card adjusts the signals to the servo amplifiers accordingly, such that the servomotors follow that path. To make sure the path is followed and the loop is closed, the motion-control card repeatedly checks the actual position of the machine's axes obtained from the encoders against the commanded position and makes adjustments to keep the difference as small as possible. The motion controller acts as the brain of the system by taking the desired target positions and motion profiles and creating the trajectories for the motors to follow.

The amplifier, developed by AMC, is a pulse width modulated (PWM) transconductance amplifier with a gain of 2.85 A/V and supply voltage requirement of 70 V. It takes the commands from the controller and generates the current required to drive or turn the motor.

The motors, manufactured by BEI, are typical "inside-out" brushless dc (BLDC) motors that provide greater output power, higher operating speeds, and cleaner and quieter operation than their brush-type counterparts. These motors are ideal for sterile environments, since there are no brushes and no particulate is discharged. Because of their inherent reliability and long-term service life, BLDC motors can significantly contribute to the lower overall cost of operation and maintenance. They turn the electrical energy into mechanical energy and produce the torque required to move the plant to the desired target position.

The Heidenhain LIP 403A encoders have a grating period of 4 μm and a maximum speed of 0.5 m/s, with a sinusoidal output. These encoders sense the motor position and report the results to the controller, thereby closing the loop to the motion controller.

Optically, a 630-nm laser source, a double slit, and an 1830-C Newport fiber receiver are being used. The receiver is a general-purpose interface bus interfaced to the computer control. The laser source is attached to the nonmoving test-bed structure, while the receiver fiber is attached to the controlled optical table. The optical power sensor reading is sent to the computer control, which controls the system for position measurement to attach at the point of the maximum power.

VI. Model-Based Control Versus Gradient Ascent Hardware Results

To highlight some of the advantages of the model-based automation process, an example is presented comparing the model-based technique with the currently used state-of-the-art control algorithms. This example pertains to the coupling of a 630-nm laser source to an optical fiber connected to an 1830-C Newport optical power meter. The laser source emits a Gaussian beam, which propagates through a double slit with slit dimensions 18×64 μm (width $\times$ length), and center-to-center separation 32 μm. This system is illustrated in Fig. 9, along with a photograph of the optical setup.

This beam is coupled to a multimode fiber. The distance between the laser source and the fiber is 1000 μm; therefore, the light has propagated only into the far field. The diffracted intensity pattern is shown in Fig. 10.

The system is first analyzed with the current state-of-the-art gradient ascent method. This process starts with an initial set point, and from this initial set point, the gradient ascent algorithm (hill-climbing) is performed to find the position alignment for the maximum power coupling into the fiber. The algorithm works by comparing the power levels at the neighboring positions and choosing the point with the higher power value. The disadvantage of this technique is that the algorithm stops at a local maximum. In this example, the power level reached using the gradient ascent technique is 0.645 μW. As seen in Fig. 10, the gradient ascent technique gets caught at a local maximum, instead of the system global maximum.

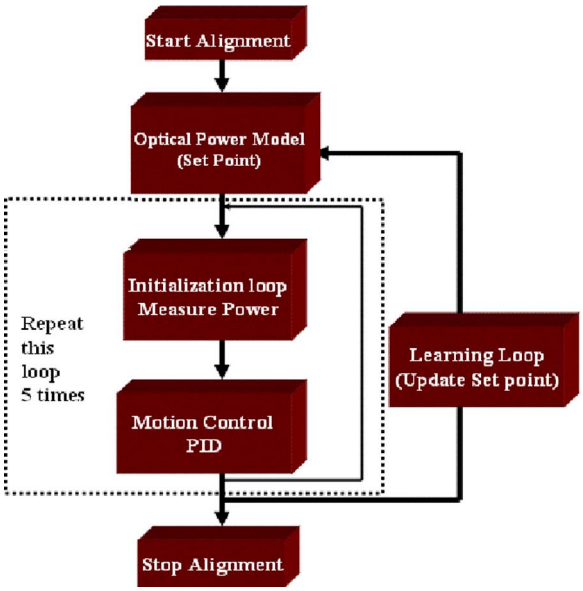

Fig. 11. Learning algorithm flowchart.

In contrast, the model-based control technique is used to determine the positional alignment for the maximum power coupled into the fiber. Therefore, we start by simulating the entire system to predict the best "feedforward" set point for the control algorithm. The simulation is performed using the angular spectrum technique, as the output intensity distribution and a distribution of the power coupled into the fiber are determined. From this "feedforward" set point, the conventional gradient ascent algorithm is performed to find the global power maximum. The power reached in this case is found to be 1.525 μW, an increase of 136% over the current state-of-the-art gradient ascent technique. A sample video demonstration of the experiment is available at http://www.ece.drexel.edu/opticslab/results/results.html.

VII. Hardware Results of the Learning Algorithm Implementation

The flowchart for implementation of the learning algorithm on the existing hardware example is shown in Fig. 11.

The initial feedforward set point is obtained from the optical power modeling done in MATLAB. This set point is given as an input to the physical medium dependent interface motion-control software, which follows a PID loop by measuring the power. Initially, a guessed value of "a" is considered, which is the center-to-center separation between the slits, as seen in Section IV. Since there are two axes to control, we have two encoder set points 10477.0 and 24.2, respectively. The inner PID loop is repeated five times after which the outer learning loop comes into effect. The learning loop updates the estimated set points and tracks to the actual set point 10810.0 and 25.0, respectively. In this simulation, the learning algorithm is run 28 times. This leads to a faster alignment and an increased power efficiency. Fig. 12 shows the tracking of the encoder set points for the X and the Y axes. A

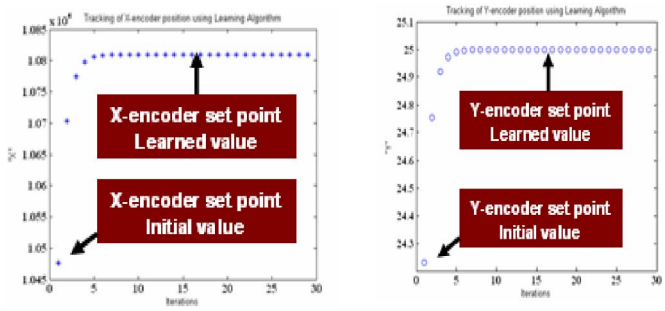

Fig. 12. X and Y encoder set points.

sample video demonstration of the experiment is available at http://www.ece.drexel.edu/opticslab/results/results.html.

VIII. Conclusion and Future Work

In this paper, a model-based automation technique is presented for optical alignment and attachment. Using this technique, we can achieve a better system performance. This technique also increases the speed of the automation process, a critical factor when many components are being packaged at the same time. Through these benefits, the overall cost of the automation process is reduced.

The focus of this paper was on a learning loop to increase the accuracy of the models, by adjusting the model based on the previous attachments or mismatches between the model and the physical performance of the system. A hardware implementation of a specific optical system was also presented, which demonstrated the advantages of the algorithm. However, this approach is a general one and can be used for all optical systems. As a future work, research is also being conducted into other learning algorithms, including simulated annealing, neural networks, fuzzy logic, and genetic algorithms.

Acknowledgment

The authors thank Kulicke and Soffa, Inc., for donating the *XY* assembly table to implement and verify the research, and M. Soffa and Z. Ahmad for their technical support.

References

[1] K. J. Astrom and B. Wittenmark, *Adaptive Control*. Reading, MA: Addison-Wesley, 1989.
[2] W. L. Brogan, *Modern Control Theory*. Surrey, U.K.: Quantum, 1974.
[3] D. D. Donaldson and C. T. Leondes, "A model referenced parameter tracking technique for adaptive control systems I and II," *IEEE Trans. Appl. Ind.*, vol. 82, pp. 241–260, Sep. 1963.
[4] R. Duer, "Lynx Photonics," private communication, Jul. 2005.
[5] M. Formica and J. Kelly, "Measure twice, attach once," *Int. Opt. Commun.*, pp. 2–4, Mar. 2002.
[6] J. W. Goodman, *Introduction to Fourier Optics*, 2nd ed. New York: McGraw-Hill, 1996.
[7] A. Guez, I. Rusnak, and I. Bar Kana, "Multiple objectives optimization approach to adaptive and learning control," *Int. J. Control*, vol. 56, no. 2, pp. 469–482, Sep. 1992.
[8] A. Guez and J. Selinsky, "Neurocontroller design via supervised and unsupervised learning," *J. Intell. Robot. Syst.*, vol. 2, pp. 307–335, 1989.
[9] B. W. Hueners and M. K. Formica, "Photon. component manufactures move towards automation," *Photon. Spectra*, pp. 66–72, Mar. 2003.

[10] S. Jang, "Automation manufacturing system technology for optoelectronic device packaging," in *Proc. 50th Electron. Compon. Technol. Conf.*, Las Vegas, NV, 2000, pp. 10–14.
[11] T. P. Kurzweg, "Optical propagation methods for system-level modeling of optical MEMS" Ph.D. disseration, Dept. Elect. Eng., Univ. Pittsburgh, Pittsburgh, PA, 2002.
[12] T. P. Kurzweg, S. P. Levitan, J. A. Martinez, M. Kahrs, and D. M. Chiarulli, "A fast optical propagation technique for modeling micro-optical systems," in *Proc. 2002 Des. Autom. Conf.*, New Orleans, LA, Jun.10–14.
[13] T. P. Kurzweg, A. Guez, and S. K. Bhat, "Model based optoelectronic packaging automation," *IEEE J. Sel. Topics Quantum Electron.*, vol. 10, no. 3, pp. 445–454, May–Jun. 2004.
[14] M. Morari and F. Zafiriou, *Robust Process Control*. Englewood Cliffs, NJ: Prentice-Hall, 1989.

Shubham K. Bhat received the M.S. degree in electrical/telecommunication engineering in 2005 from Drexel University, Philadelphia, PA, where he is currently working toward the Ph.D. degree in electrical engineering.

His current research interests include control systems theory, optimal control, system identification, parameter estimation, system-level optical modeling, and optoelectronic packaging.

Mr. Bhat is a Student Member of the IEEE Lasers and Electro-Optics Society.

Timothy P. Kurzweg (S'92–M'95) received the B.S. degree from Pennsylvania State University, University Park, in 1994, and the M.S. and Ph.D. degrees from the University of Pittsburgh, Pittsburgh, PA, in 1997 and 2002, respectively, all in electrical engineering.

He is an Assistant Professor in the Department of Electrical and Computer Engineering, Drexel University, Philadelphia, PA. During 1999, he worked with Microcosm (now Coventor), Cambridge, MA, and developed an optical methodology to interface with a system-level analysis tool enabling optical microelectromechanical simulation (MEMS). His current research interests include modeling and simulation, optical MEMS, computer-aided design, free-space optics, very large-scale integration, and computer architecture.

Dr. Kurzweg is a member of the IEEE Lasers and Electro-Optics Society, the Association for Computer Machinery/Special Interest Group on Design Automation, and the Optical Society of America.

Allon Guez received the B.S. and M.S. degrees in electrical engineering from The Technion— Israel Institute of Technology, Haifa, Israel, in 1978 and 1980, respectively. He received the Ph.D. degree in electrical engineering from the University of Florida, Gainesville, in 1983, and the MBA degree in finance from Drexel University, Philadelphia, PA, in 1996.

He is currently a Professor of Electrical and Computer Engineering and the Director of Drexel University's Robotics and Automation Laboratory. As a Consultant, he frequently advises industry. He is the author or coauthor of more than 200 technical publications and patents. His current research interests include control systems, automation, distributed online decision making, business systems engineering, and biomorphic algorithms and architectures.